Research Article

Phase-Only Antenna Array Reconfigurability with Gaussian-Shaped Nulls for 5G Applications

Giulia Buttazzoni [ID]**, Massimiliano Comisso** [ID]**, Federico Ruzzier, and Roberto Vescovo** [ID]

Department of Engineering and Architecture, University of Trieste, Via A. Valerio 10, 34127 Trieste, Italy

Correspondence should be addressed to Giulia Buttazzoni; gbuttazzoni@units.it

This paper presents a fast iterative method for the synthesis of linear and planar antenna arrays of arbitrary geometry that provides pattern reconfigurability for 5G applications. The method enables to generate wide null regions shaped according to a Gaussian distribution, which complies with recent measurements on millimeter-wave (mmWave) angular dispersion. A phase-only control approach is adopted by moving from the pattern provided by a uniformly excited array and iteratively modifying the sole phases of the excitations. This allows the simplification of the array feeding network, hence reducing the cost of realization of 5G base stations and mobile terminals. The proposed algorithm, which is based on the method of successive projections, relies on closed-form expressions for both the projectors and the null positions, thus allowing a fast computation of the excitation phases at each iteration. The effectiveness of the proposed solution is checked through numerical examples compliant with 5G mmWave scenarios and involving linear and concentric ring arrays.

1. Introduction

By now, the expected outbreak of the 5G technology represents one of the main challenging opportunities for antenna designers, whose efforts will have to deal with several significant designs, realizations, and prototyping issues. One of the distinctive features of next-generation cellular systems will in fact consist in the adoption of the millimeter-wave (mmWave) spectrum, between 30 and 300 GHz, to satisfy the huge capacity demand that will require the implementation of the Internet of Things (IoT) and Internet of Everything (IoE) paradigms [1]. The main reasons that have driven the attention of the 5G developers towards the extremely high-frequency (EHF) band are the considerable amount of unused bandwidth and the possibility of packaging many radiating elements in a single mobile terminal (MT) or base station (BS), with the aim of providing a high gain, so as to compensate the significant attenuation of the mmWave channel. For the first time, from the deployment of the previous 1-4G systems, the 5G network will indeed have to necessarily rely on beamforming both in transmission and reception, to make the communications feasible in a propagation environment much more sensitive to blockages due to obstacles [2–4].

In this context, a basic approach to find the most suitable beamforming techniques for mmWave links may be that of considering the significant amount of algorithms that have been developed along the years and that gave outstanding solutions for a wide variety of synthesis problems. To make a preliminary effective selection, it may be also useful to properly identify the main antenna requirements that are expected to characterize the forthcoming 5G transceivers. Firstly, since mmWave systems will be designed to manage a dense environment, the spatial filtering capabilities of the antenna array will represent the main topic, to the point that many studies have assumed a significant change of perspective for the analytical characterization of the 5G performance, consisting in the translation from the so far assumed 1-4G interference-limited regime to a 5G noise-limited one [5]. In this scenario, the shape of the pattern and, precisely, its beamwidth and side-lobe level (SLL), as well as the depth and width of its possible nulls, will play a key role for the sustainability of the 5G links. A second relevant antenna requirement concerns the feeding network.

Since the significant mmWave attenuations will force the developers to adopt small cells, a huge number of BSs is expected to be deployed. This leads to the need of containing the fabrication costs not only of the MTs but also of the BSs and, in turn, of the corresponding antenna systems, thus orienting the choice of the beamforming algorithm towards a phase-only control approach, which leads to a simplified feeding network.

In light of these considerations, this paper proposes a fast synthesis algorithm for linear and planar antenna arrays of arbitrary geometry that allows the reconfigurability of the pattern and the shaping of the null regions according to a Gaussian power azimuth spectrum. The algorithm takes, as starting point, a uniformly excited array, which provides a narrow beamwidth, and then iteratively modifies the sole phases of the excitations to impose wide Gaussian nulls in specified directions. Furthermore, the algorithm, which relies on the method of successive projections, is developed to obtain closed-form expressions for the projectors and analytical formulas for the positions of the nulls. This approach has the advantage of leading to a fast computation of the excitation phases, since no numerical estimations are required at each iteration. Numerical examples considering linear and concentric ring arrays are presented to assess the effectiveness of the proposed solution in a 5G interfered context, discussing, beside the performance in terms of obtained patterns, also the computational time necessary for their synthesis.

The paper is organized as follows. Section 2 presents the related work. Section 3 formulates the problem. Section 4 describes the development of the algorithm. Section 5 discusses the numerical results. Section 6 summarizes the most relevant conclusions.

2. Related Work

Many phase-only null synthesis techniques for antenna arrays proposed in the recent years [6–18] may be nowadays reconsidered for addressing the expected 5G requirements. In particular, a deterministic method for linear arrays is presented in [6], where the phase-only approach and the possibility to generate multiple close nulls are outlined. Two iterative solutions for arbitrary arrays are derived [7], with the aim of exploiting a root mean square approximation to enable null synthesis by phase-only control. In [8], the problem of assigning prescribed nulls in the pattern of a linear array by phase-only control is solved through the development of a genetic algorithm. A phase-only null synthesis method for linear arrays is also discussed in [9], where the authors adopt a sequential quadratic programming approach. Scenarios specifically considering the phase-only synthesis of wide nulls for arrays of arbitrary geometry are addressed in [10], by taking into account the power azimuth spectrum of the interferers. In [11], a beamforming architecture based on neural networks is designed to introduce phase-only adaptive nulling in phased arrays. The synthesis of cylindrical arc antenna arrays controlled by the excitation phases is analyzed in [12], where the null steering capabilities are experimentally proved through a prototype consisting of

microstrip patches. In [13], the authors propose a differential search optimization algorithm for linear arrays, which includes the phase-only control and wide null synthesis options. The same options are enabled in [14], which alternatively applies a metaheuristic backtracking search optimization approach based on an iterative process controlled by a single parameter. The method of alternate projections is adopted in [15], to develop an iterative algorithm for null synthesis problems in arrays of arbitrary geometry, which includes the possibility of imposing the phase-only constraint. In [16], a phase-only beamformer based on the adaptive bat algorithm is designed to impose nulls in a certain number of undesired directions when a uniformly spaced linear array of half-wave dipoles is employed. In [17], a powerful method for the reconfigurability and beam scanning with phase-only control for arbitrary antenna arrays is presented, which also allows to form wide deep nulls. The method is based on a smart application of the alternate projection approach. A versatile solution is presented in [18], where a weighted cost function is used to impose multiple synthesis requirements, including phase-only control and null steering for conformal antenna arrays.

With reference to this overview, some common aspects may be highlighted. First, the phase-only requirement during the null synthesis process implies the maintenance of a unity dynamic range ratio (DRR), representing the ratio between the maximum and the minimum excitation amplitudes of the array. The problem of forming nulls while imposing an upper bound on the DRR has been discussed in detail in [19], where a theorem providing a necessary and sufficient condition for the joint application of null and DRR constraints on any array geometry is mathematically proved. In particular, it has been statistically shown that, if the number of required nulls is small compared to the number of array elements, such condition is typically satisfied also for unity DRR, thus allowing to form exact nulls (and a fortiori deep nulls) by phase-only control, which is here the case of main interest.

Second, many of the proposed solutions are applicable just to specific configurations [6, 8, 9, 11–14, 16], usually having a linear geometry. However, planar structures are expected to be used for 5G MTs and BSs [2], thus an algorithm capable to operate on conformal structures may be highly preferable.

Third, the recent channel measurements carried out at the mmWave frequencies have revealed that the angular dispersion may be often described by a Gaussian distribution [20, 21], thus better identifying the shape of the wide nulls that may be necessary to suppress the undesired sources. Currently, none of the existing methods combines wide nulling and Gaussian shaping together with a low computation time, which represents a not negligible requirement for 5G cellular systems, whose operations will have to necessarily adopt fast beamforming solutions. The specific case of Gaussian null shaping is considered in [10], but passing through a numerical estimation of the position of the nulls, which does not rely on closed-form expressions, and hence may become computationally cumbersome.

For these reasons, in this paper, we present a phase-only control algorithm for arbitrary linear and planar arrays capable of managing Gaussian-distributed nulls. Moving from the

formulation of the problem developed in the next section, the algorithm is mathematically derived in Section 4.

3. Problem Formulation

With reference to a Cartesian system $O(x, y, z)$, consider an antenna array of N elements lying on the yz-plane, where the position of the n-th element is specified by the vector $\bar{\mathbf{d}}_n = x_n \hat{\mathbf{x}} + y_n \hat{\mathbf{y}} + z_n \hat{\mathbf{z}}$ (denoting by $\hat{\mathbf{x}}$, $\hat{\mathbf{y}}$, and $\hat{\mathbf{z}}$ the unit vectors of the Cartesian coordinate axes x, y, and z, respectively). In the generic space direction $\hat{\mathbf{r}}$, the radiation pattern of this array is given by

$$P(\mathbf{i} ; \hat{\mathbf{r}}) = \sum_{n=1}^{N} i_n p_n(\hat{\mathbf{r}}) \exp \left(j\beta \bar{\mathbf{d}}_n \cdot \hat{\mathbf{r}} \right), \tag{1}$$

where $\mathbf{i} = [i_1, \ldots, i_N]^T$ is the column vector of the complex excitations, $p_n(\hat{\mathbf{r}})$ is the n-th array element pattern, $\beta = 2\pi/\lambda$ is the wave number, with λ denoting the wavelength, j is the imaginary unit, and $\hat{\mathbf{r}} = \sin \theta \cos \phi \hat{\mathbf{x}} + \sin \theta \sin \phi \hat{\mathbf{y}} + \cos \theta \hat{\mathbf{z}}$, with $\phi \in [-\pi, \pi$ and $\theta \in [0, \pi]$ denoting the azimuth and zenith angles, respectively. In the sequel, for more simplicity, we will assume that the direction of observation belongs to the xy-plane, so that (1) can be expressed as a function of the azimuth angle as follows:

$$P(\mathbf{i} ; \phi) = \sum_{n=1}^{N} i_n p_n(\phi) \exp \left(j\beta y_n \sin \phi \right). \tag{2}$$

Consider now a reference pattern $P_0 = P(\mathbf{i}_0 ; \phi)$, with the main beam pointing at a desired direction ϕ_0, and an interferer whose angle of arrival (AoA) is statistically described by a truncated Gaussian distribution having probability density function (pdf):

$$f_g(\phi) = \frac{Q_L}{\sigma \sqrt{2\pi}} \exp \left[-\frac{(\phi - \bar{\phi})^2}{2\sigma^2} \right] 1_{[-\pi, \pi)}(\phi), \tag{3}$$

where Q_L is a constant that imposes the normalization condition $\int_{-\pi}^{\pi} f_g(\phi) d\phi = 1$, σ is the standard deviation, which can be inferred from experimental measurements in the mmWave channel [20, 21], $\bar{\phi}$ is the mean AoA, and $1_{\mathbf{X}}(\mathbf{x})$ denotes the indicator function (that is, $1_{\mathbf{X}}(\mathbf{x}) = 1$ if $\mathbf{x} \in \mathbf{X}$ and $1_{\mathbf{X}}(\mathbf{x}) = 0$ if $\mathbf{x} \notin \mathbf{X}$).

According to this scenario, the objective of this study is to find a pattern $P = P(\mathbf{i} ; \phi)$ that solves the following minimization problem:

$$\min_{\mathbf{i}} \quad \|P - P_0\|^2 \tag{4}$$

$$\text{subject to} \quad |i_n| = |i_{0n}|, \; n = 1, \ldots, N \tag{5}$$

$$|P(\mathbf{i} ; \phi)| \leq Q f_g(\phi), \quad \phi \in [\phi_l, \phi_u], \tag{6}$$

where $\mathbf{i}_0 = [i_{01}, \ldots, i_{0N}]^T$, $\|\cdot\|$ is a suitable norm, Q is a constant taking into account the amplitude of the interferer,

and $[\phi_l, \phi_u]$ identifies the angular region of interest. Note that the constraint in (5) means that only the excitation phases of $\mathbf{i}_0$ are modified.

4. The Solving Procedure

The adopted synthesis strategy starts by substituting the wide null constraint in (6) with the following M single null constraints:

$$P(\mathbf{i} ; \phi_m) = 0, \quad m = 1, \ldots, M, \tag{7}$$

that is, imposing that the pattern vanishes at the directions $\phi_1, \ldots, \phi_M$. In matrix form, (7) can be expressed as follows:

$$\mathbf{E}\mathbf{i} = 0, \tag{8}$$

where $\mathbf{E} = [E_{mn}]$, with $E_{mn} = p_n(\phi_m) \exp \left(j\beta y_n \sin \phi_m \right)$ for $m = 1, \ldots, M$ and $n = 1, \ldots, N$. As shown in [10], a proper choice of the null positions allows one to satisfy the initial constraint in (6) by reformulating the original problem to an equivalent one solvable in a simple and very fast way. The derived solution is illustrated in the sequel of this section. More precisely, the strategy to suitably select the M null directions is described in the following subsection, while the procedure of phase-only M null synthesis is presented in Section 4.2.

4.1. Null Positioning. The localization of the nulls is performed here by a density tapering technique, which consists in finding the M null directions by imposing an equiareal requirement as follows:

$$\int_{-\pi}^{\phi_1} f_g(\phi) d\phi = \int_{\phi_1}^{\phi_2} f_g(\phi) d\phi = \cdots = \int_{\phi_M}^{\pi} f_g(\phi) d\phi. \tag{9}$$

Since $\int_{-\pi}^{\pi} f_g(\phi) d\phi = 1$, each integral in (9) must be equal to $1/(M + 1)$. Hence, imposing $\int_{-\pi}^{\phi_m} f_g(\phi) d\phi = m/(M + 1)$ for $m = 1, \ldots, M$, after some manipulations, one obtains [22]

$$\phi_m = \sqrt{2}\sigma \; \mathrm{erf}^{-1} \left[\frac{2m}{Q_L(M + 1)} + \mathrm{erf} \left(-\frac{\pi + \bar{\phi}}{\sqrt{2}\sigma} \right) \right] + \bar{\phi}, \tag{10}$$

where $\mathrm{erf}\,(x)$ denotes the error function and $\mathrm{erf}^{-1}(x)$ represents its inverse. In this way, the nulls, whose position is available in analytical form, are more dense near the mean value $\bar{\phi}$, where the pdf is higher, and less dense far from $\bar{\phi}$, where the pdf is lower. Once the null directions are evaluated by (10), the reformulated problem is then solved by the alternating projection approach, as described in detail in the next subsection.

4.2. Phase-Only Null Synthesis by Alternating Projections. In order to model the synthesis problem as an intersection finding problem, first denote $\mathscr{P}$ as the set of all the patterns that can be generated by the considered array. Then, in $\mathscr{P}$, introduce a set $\mathscr{H}$, composed by all the patterns that are produced by an excitation vector that satisfies constraint (5), and a set

$\mathscr{Z}$, composed by all the patterns that satisfy constraint (7). It is evident that a radiation pattern belonging to both sets $\mathscr{H}$ and $\mathscr{Z}$ (if any), and having the minimum distance from P_0, is a solution to our (reformulated) problem, since it satisfies (4), (5), and (7). Thus, a point very close to P_0 and belonging to the intersection of the two sets is sought. If $\mathscr{H} \cap \mathscr{Z}$ is empty, such a point does not exist, and we search for a point of $\mathscr{H}$ having the minimum distance from $\mathscr{Z}$, so as to obtain deep nulls by phase-only control. To this aim, adopting the alternating projection approach [17, 23], an iterative procedure is performed by starting from the reference pattern $P_0 \in \mathscr{H}$ and then following the scheme:

$$P_n = T_{\mathscr{H}} T_{\mathscr{Z}} P_{n-1}, \quad n = 1, 2, 3, \ldots , \tag{11}$$

where $P_{\mathscr{H}}$ and $P_{\mathscr{Z}}$ denote the projection operators onto the sets $\mathscr{H}$ and $\mathscr{Z}$, respectively. Each pattern of the sequence $\{P_n\}$ belongs to the set $\mathscr{H}$; thus, it satisfies the phase-only requirement, and is closer and closer to the set $\mathscr{Z}$, due to a well-known property of the alternating projection method, $\|P_n - T_{\mathscr{Z}} P_n\| \geq \|P_{n+1} - T_{\mathscr{Z}} P_{n+1}\|$ for each $n \geq 1$. The iterations are stopped at a point $P_n \in \mathscr{H}$ such that

$$\begin{aligned} d_n &< \varepsilon_1 \\ \text{or } \frac{d_{n-1} - d_n}{d_n} &< \varepsilon_2, \end{aligned} \tag{12}$$

where d_n is the distance between the pattern P_n and the set $\mathscr{Z}$, while ε_1 and ε_2 are proper positive thresholds.

It is worth noting that the iteration is stopped at a point of $\mathscr{H}$; thus, the constraint in (5) is rigorously satisfied, and hence phase-only control is achieved. In general, $P_n \notin \mathscr{Z}$; thus, the null constraints in (7) are not exactly satisfied, but sufficiently deep nulls are achieved after a suitable number of iterations. Hence, the constraints in (7) and, in turn, the original one in (6), are approximated very well. Since the starting point is P_0, the alternating projection approach provides a point close to P_0, approximately satisfying (4) and simultaneously satisfying (5) (exactly) and (7) (approximately). This objective is achieved by properly defining the projectors $T_{\mathscr{H}}$ and $T_{\mathscr{Z}}$ in (11), whose mathematical derivation is described in detail in the next paragraphs.

4.2.1. The Projector $T_{\mathscr{H}}$. The algorithm for this projector is described here following the procedure in Section V of [19]. Projecting an array pattern $P(\mathbf{i}_x ; \phi)$ onto the set $\mathscr{H}$ requires to find an array pattern $P(\mathbf{i} ; \phi) \in \mathscr{H}$ minimizing the distance:

$$\delta(\mathbf{i}) = \|P(\mathbf{i} ; \phi) - P(\mathbf{i}_x ; \phi)\|. \tag{13}$$

The distance in (13) is defined by means of the norm $\|f(\phi)\| = \sqrt{<f, f>}$, involving the scalar product $\langle f, g \rangle = \int_{-\pi}^{\pi} f(\phi) g^*(\phi) d\phi$, where the asterisk denotes the complex conjugate. Substituting (2) into (13), after some manipulations, one obtains

$$\delta^2(\mathbf{i}) = (\mathbf{i} - \mathbf{i}_x)^H \mathbf{G}(\mathbf{i} - \mathbf{i}_x) = \sum_{m=1}^{N} (i_m^* - i_{xm}^*) \sum_{n=1}^{N} G_{mn}(i_n - i_{xn}), \tag{14}$$

where the superscript H denotes the transposed conjugate and $\mathbf{G} = [G_{mn}]$ is an $N \times N$ matrix whose generic element is given by

$$G_{mn} = \langle p_n(\phi) \exp (j\beta y_n \sin \phi), p_m(\phi) \exp (j\beta y_m \sin \phi)\rangle, \tag{15}$$

for $m, n = 1, \ldots , N$. Since the unknown pattern has to belong to the set $\mathscr{H}$, it must satisfy constraint (5). Thus, we set

$$i_n = \rho_{0n} \exp (j\alpha_n), \tag{16}$$

where $\rho_{0n} = |i_{0n}|$ for $n = 1, \ldots , N$. Substituting (16) into (14) and putting the generic p-th term into evidence, yields

$$\begin{aligned} \delta^2(\mathbf{i}) = G_{pp} \left| \rho_{0p} \exp (j\alpha_p) - i_{xp} \right|^2 + H_p \left[\rho_{0p} \exp (-j\alpha_p) - i_{xp}^* \right] \\ + H_p^* \left[\rho_{0p} \exp (j\alpha_p) - i_{xp} \right] + K_p, \end{aligned} \tag{17}$$

where

$$\begin{aligned} H_p &= \sum_{n \neq p} G_{pn} [\rho_{0n} \exp (j\alpha_n) - i_{xn}], \\ K_p &= \sum_{m \neq p} [\rho_{0m} \exp (-j\alpha_m) - i_{xm}^*] \times \sum_{n \neq p} G_{mn} [\rho_{0n} \exp (j\alpha_n) - i_{xn}]. \end{aligned} \tag{18}$$

The unknown phases are found following the single coordinate method (SCM) [7], beginning from the phases of the excitations of the reference pattern. Accordingly, at each step the $N - 1$ variables $\alpha_1, \ldots , \alpha_{p-1}, \alpha_{p+1}, \ldots , \alpha_N$ are considered as known, and the value of the unknown α_p that minimizes (17) is obtained by imposing the vanishing of the derivative of $\delta^2(\mathbf{i})$ with respect to α_p. This yields

$$\alpha_p = \arg (S_p) + k\pi, \quad k = 0, \pm 1, \pm 2, \ldots , \tag{19}$$

where

$$S_p = \rho_{0p} (G_{pp} i_{xp} - H_p). \tag{20}$$

Calculating (19) for $p = 1, \ldots , N$ and repeating the iteration for a sufficient number of times yield the unknown phases, which, once substituted in (16), give the required excitation vector. Substituting the latter into (2) gives the radiation pattern $P(\mathbf{i} ; \phi)$, projection of $P(\mathbf{i}_x ; \phi)$ onto $\mathscr{H}$.

4.2.2. The Projector $T_{\mathcal{Z}}$. The algorithm for this projector has been illustrated in [24] for the case of nulls in the near-field region. It is described here in detail for the case of nulls in the far-field region, which is of interest for the presently addressed scenario. Given any pattern $P(\mathbf{i}_x; \phi)$, the pattern $P(\mathbf{i}; \phi) = T_{\mathcal{Z}} P(\mathbf{i}_x; \phi)$, projection of $P(\mathbf{i}_x; \phi)$ onto $\mathcal{Z}$, is the pattern that minimizes the squared distance (14) subject to the constraints (7). Here, we note that the matrix $\mathbf{G}$ in (14) is Hermitian. Therefore, it can be written as follows:

$$\mathbf{G} = \mathbf{U}^H \mathbf{\Lambda} \mathbf{U}, \tag{21}$$

where $\mathbf{\Lambda}$ is a diagonal matrix whose diagonal elements are the eigenvalues of $\mathbf{G}$, while $\mathbf{U}$ is a unitary matrix whose rows are the (orthonormal) eigenvectors corresponding to the eigenvalues. Substituting (21) into (14) and setting $\mathbf{w} = \mathbf{\Lambda}^{1/2} \mathbf{U} \mathbf{i}$ and $\mathbf{w}_x = \mathbf{\Lambda}^{1/2} \mathbf{U} \mathbf{i}_x$ yield

$$\delta^2(\mathbf{i}) = (\mathbf{w} - \mathbf{w}_x)^H (\mathbf{w} - \mathbf{w}_x). \tag{22}$$

On the other hand, being $\mathbf{w} = \mathbf{\Lambda}^{1/2} \mathbf{U} \mathbf{i}$ we can write $\mathbf{i} = \mathbf{K}\mathbf{w}$, where $\mathbf{K} = \mathbf{U}^H \mathbf{\Lambda}^{-1/2}$. Thus, the constraints in (7) and (8) can be written as $\mathbf{S}\mathbf{w} = 0$, where $\mathbf{S} = \mathbf{E}\mathbf{K}$. Therefore, the problem of projecting $P(\mathbf{i}_x; \phi)$ onto $\mathcal{Z}$ reduces to that of determining the column vector $\mathbf{w}$ that minimizes (22) subject to condition $\mathbf{S}\mathbf{w} = 0$. As it is well known, this problem has the solution $\mathbf{w} = (\mathbf{I}_N - \mathbf{S}^\dagger \mathbf{S})\mathbf{w}_x$, where $\mathbf{I}_N$ is the $N \times N$ identity matrix and $\mathbf{S}^\dagger$ is the pseudoinverse of $\mathbf{S}$. Being $\mathbf{w}_x = \mathbf{\Lambda}^{1/2} \mathbf{U} \mathbf{i}_x$, it results

$$\mathbf{i} = \mathbf{P}_{\mathcal{Z}} \mathbf{i}_x, \tag{23}$$

where

$$\mathbf{P}_{\mathcal{Z}} = \mathbf{K}(\mathbf{I}_N - \mathbf{S}^\dagger \mathbf{S})\mathbf{\Lambda}^{1/2}\mathbf{U}. \tag{24}$$

The column vector $\mathbf{i}$ in (23) provides the complex excitations, which, once inserted in (2) give the projected array pattern $P(\mathbf{i}; \phi) = T_{\mathcal{Z}} P(\mathbf{i}_x; \phi)$.

Now that the projectors have been derived, the iterative procedure in (11) with starting point P_0 can be carried out to solve the original phase-only synthesis problem with Gaussian-shaped null in (4)–(6). The performances achievable by this method are investigated in the next section.

5. Numerical Results

In this section, two numerical examples are proposed to assess the validity of the proposed procedure. The two examples are also solved with the first method developed in [7], which can perform phase-only null synthesis for arbitrary arrays and is hence suitable for comparison with that proposed in this paper. Both the synthesis methods are implemented in MATLAB R2015b, and all results are obtained using a laptop equipped with an Intel® Core™ i5-5300U CPU @ 2.30 GHz with 8 GB RAM.
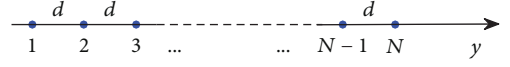

FIGURE 1: First example: geometry of the linear array with $N = 40$ elements and interelement distance $d = \lambda/2$.
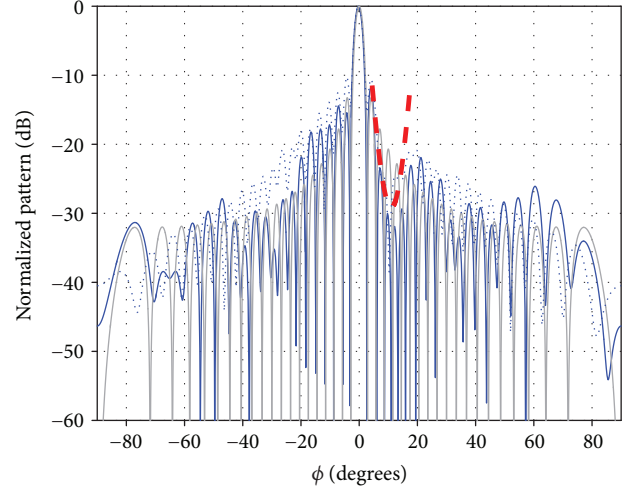

FIGURE 2: First example: linear array in Figure 1. Thin gray line: reference pattern. Thick solid blue line: pattern synthesized using the proposed algorithm. Thick dotted blue line: pattern synthesized using the algorithm proposed in [7]. Dashed red line: local upper bound of constraint (6).

5.1. First Example: Linear Array of Omnidirectional Elements. The first numerical example refers to a phase-only synthesis problem for a linear array consisting of $N = 40$ elements equally spaced along the y-axis (Figure 1). The interelement distance is $d = \lambda/2$. The element patterns $p_n(\phi)$ are assumed to be equal and omnidirectional on the xy-plane (this can be the case of an array consisting of half-wavelength dipoles parallel to the z-axis), that is, $p_n(\phi) = 1$ for $n = 1, \ldots, N$ and $\phi \in [-\pi, \pi]$. The reference pattern, which is represented by the gray line in Figure 2, is produced by this array with uniform excitations, that is, by setting, in (2), $i_n = 1$ and $y_n = n d$ for $n = 1, \ldots, N$. An interferer is assumed to act very close to the pointing direction $(\phi_0 = 0°)$ and is characterized by the truncated Gaussian pdf in (3) with $\bar{\phi} = 11°$ and $\sigma = 9°$. The solving procedure described in the previous section is applied adopting $M = 7$ null directions evaluated by (10).

The obtained pattern is represented in Figure 2 by the blue thick line, while the dotted blue line represents the pattern synthesized by the algorithm in [7], and the dashed red line identifies the upper bound corresponding to the pdf of the Gaussian interferer. An enlargement of the synthesized patterns in the null region is reported in Figure 3. This first example shows that, with respect to the starting reference pattern, approximately a 10 dB reduction in the region of interest is achieved by the proposed method. Besides, this reduction is obtained by properly shaping the wide null region according to the desired Gaussian pdf, thus confirming the suitability of the replacement of the original constraint in (6) with the M null one in (7). Of course, this reduction (as any imposed constraint) may cause
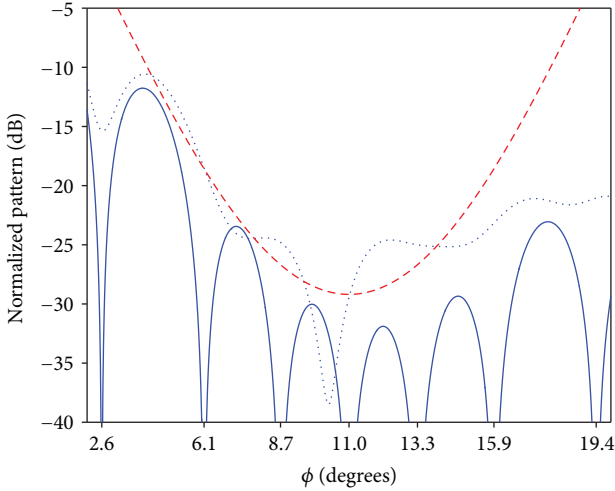
FIGURE 3: Magnification of the pattern synthesized in Figure 2 in the interference region with the evaluated null positions. To be noted that the constraint (6) is satisfied rigorously with the presented procedure and approximately with the method proposed in [7]. Also, it is to be noted that the pattern amplitude on the $M = 7$ null directions evaluated according to (10) is extremely low.
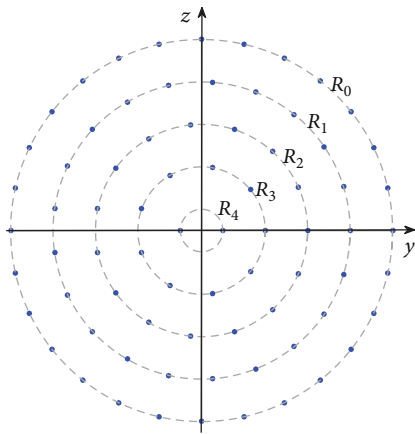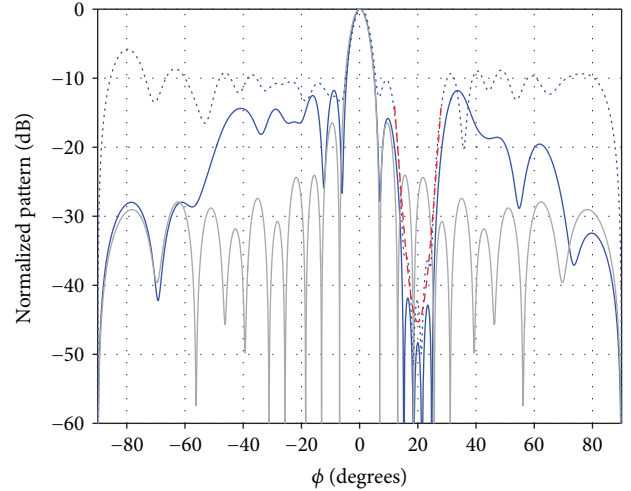

FIGURE 5: Second example: circular array in Figure 4. Thin gray line: reference pattern. Thick solid blue line: pattern synthesized using the proposed algorithm. Thick dotted blue line: pattern synthesized using the algorithm proposed in [7]. Dashed red line: local upper bound of constraint (6).

FIGURE 4: Second example: geometry of the circular array with five rings of $N = 75\cos\phi$ elements, represented by the blue dots on the yz-plane.
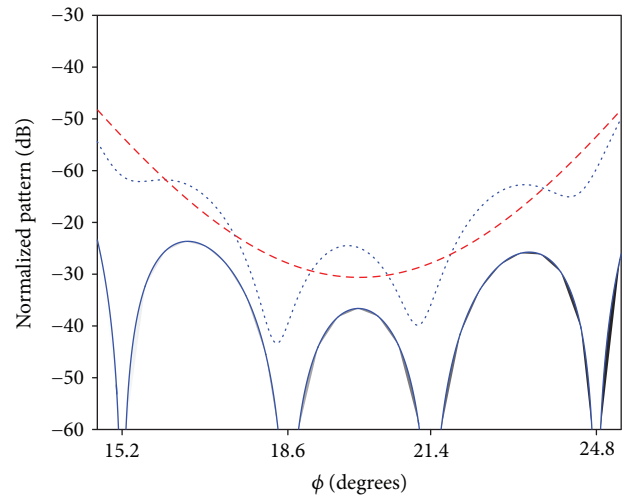

FIGURE 6: Magnification of the synthesized pattern in Figure 5 in the interference region with the evaluated null positions. Also, in this case, the original constraint (6) is satisfied rigorously by the pattern synthesized with the presented method and the pattern amplitude on the $M = 4$ null directions evaluated according to (10) is extremely low.

modifications in other angular regions of the reference pattern. In particular, in this first example, the most significant changes for the proposed method with respect to the reference pattern are a slight increase of the side lobe between the main beam and the imposed Gaussian null (which is not surprising) and an increase of the side lobes in the intervals $[60°, 80°]$, both balanced by a decrease of the side lobes in the opposite directions. However, we may notice that the pattern modification obtained with the method in [7] is much more relevant on the entire angular domain. It is also worth to observe that the synthesis of the final pattern has required slightly less than half second of computational time, corresponding to just 22 iterations with the proposed algorithm here, and 992 s, corresponding to 1000 iterations, with the method in [7].

5.2. Second Example: Planar Circular Array with Multiple Rings and cos Φ Element Patterns.
The second numerical example deals with the phase-only synthesis of a Gaussian null region using a planar array involving $N_r = 5$ concentric rings lying on the yz-plane. The radius of the outermost ring is $R_0 = 4.5\lambda$. The other radii are $R_i = R_0 - i\lambda$ for $i = 1, 2, 3, 4$. On the i-th ring, N_i elements are equally spaced so as to give an interelement distance not lower than λ. Precisely, the rings consist of $N_0 = 28$, $N_1 = 21$, $N_2 = 15$, $N_3 = 9$, and $N_4 = 2$ elements, resulting in a total number $N = 75$ elements. The

TABLE 1: Comparison of the results.

		Iteration number	CPU time (s)	Constraint (6) satisfied
Example 1	Proposed algorithm	22	0.5	Rigorously
	Algorithm in [7]	1000	992	Approximately
Example 2	Proposed algorithm	75	0.7	Rigorously
	Algorithm in [7]	1000	2236	No

geometry of this planar array is shown in Figure 4. The element patterns are assumed to be equal to $p_n(\phi) = \cos \phi$ for $n = 1, \dots, N$ and $\phi \in [-\pi, \pi$, which models the case of microstrip patches lying on the yz-plane. The reference pattern, corresponding to equal excitations, is still reported in gray in Figure 5, while the Gaussian interferer is characterized by a pdf with $\bar{\phi} = 20°$ and $\sigma = 7°$. The results are derived by adopting $M = 4$ null directions in (10).

The synthesized pattern is denoted in Figure 5 by the blue thick line, while the dotted blue line represents the pattern synthesized by the algorithm in [7], and the dashed red line represents the truncated Gaussian pdf. The magnification of the null region is shown in Figure 6. This second example confirms the satisfactory results provided by the proposed algorithm, also in comparison with the method in [7]. In particular, in this case, with respect to the starting pattern, a 20 dB reduction is achieved, while properly shaping the region of interest. Moreover, similarly to the previous example, also for this planar geometry, the computational time remained lower than one second (precisely 0.7 s) with the proposed algorithm, whereas 2236 s (1000 iterations) were necessary with the method in [7]. Table 1 finally summarizes the computational times and the satisfied constraints for the two compared methods.

6. Conclusions

An efficient technique has been proposed for the phase-only synthesis of antenna arrays with wide null regions characterized by a Gaussian shape. The synthesis algorithm has been derived by exploiting the alternating projection approach, in which all the operations are carried out in closed form. Thus, despite the iterative nature of the alternating projections, the overall synthesis procedure results extremely fast, so that the proposed algorithm can be suitable for 5G beamforming applications, where fast synthesis algorithms are recommended. Furthermore, the degrees of freedom of the problem seem to be exploited quite satisfactorily. In fact, the phase-only synthesis has been realized by moving from a uniform amplitude distribution of the array excitations, thus modifying just the phases of the element excitations. This results in a very simple feeding network, requiring only phase shifters, which are cheap and fast components. The effectiveness of the developed synthesis strategy has been verified by numerical examples involving linear and planar arrays, which have proved the low computational time required by the developed algorithm and its significant performance in terms of null region shaping and deepening.

Data Availability

All the data necessary to obtain the results presented in Section 5 (Numerical Results) can be found by the reader in the manuscript.

Conflicts of Interest

The authors declare that there is no conflict of interest regarding the publication of this paper.

References

[1] J. G. Andrews, S. Buzzi, W. Choi et al., "What will 5G be?," *IEEE Journal on Selected Areas in Communications*, vol. 32, no. 6, pp. 1065–1082, 2014.

[2] M. R. Akdeniz, Y. Liu, M. K. Samimi et al., "Millimeter wave channel modeling and cellular capacity evaluation," *IEEE Journal on Selected Areas in Communications*, vol. 32, no. 6, pp. 1164–1179, 2014.

[3] J. F. Monserrat, S. Inca, J. Calabuig, and D. Martín-Sacristán, "Map-based channel model for urban macrocell propagation scenarios," *International Journal of Antennas and Propagation*, vol. 2015, Article ID 172501, 5 pages, 2015.

[4] H. Jung and I.-H. Lee, "Connectivity analysis of millimeter-wave device-to-device networks with blockage," *International Journal of Antennas and Propagation*, vol. 2016, Article ID 7939671, 9 pages, 2016.

[5] S. Singh, R. Mudumbai, and U. Madhow, "Interference analysis for highly directional 60-GHz mesh networks: the case for rethinking medium access control," *IEEE/ACM Transactions on Networking*, vol. 19, no. 5, pp. 1513–1527, 2011.

[6] H. Steyskal, R. Shore, and R. Haupt, "Methods for null control and their effects on the radiation pattern," *IEEE Transactions on Antennas and Propagation*, vol. 34, no. 3, pp. 404–409, 1986.

[7] A. D. Khzmalyan and A. S. Kondrat'yev, "Fast iterative methods for phase-only synthesis of antenna array pattern nulls," *Electronics Letters*, vol. 31, no. 8, pp. 601-602, 1995.

[8] R. L. Haupt, "Phase-only adaptive nulling with a genetic algorithm," *IEEE Transactions on Antennas and Propagation*, vol. 45, no. 6, pp. 1009–1015, 1997.

[9] M. Mouhamadou, P. Vaudon, and M. Rammal, "Smart antenna array patterns synthesis: null steering and multi-user beamforming by phase control," *Progress In Electromagnetics Research*, vol. 60, pp. 95–106, 2006.

[10] M. Comisso and R. Vescovo, "Exploitation of spatial channel model for antenna array synthesis," *Electronics Letters*, vol. 42, no. 19, pp. 1079-1080, 2006.

[11] R. Ghayoula, N. Fadlallah, A. Gharsallah, and M. Rammal, "Phase-only adaptive nulling with neural networks for antenna

array synthesis," *IET Microwaves, Antennas & Propagation*, vol. 3, no. 1, pp. 154–163, 2009.

[12] H. Rammal, C. Olleik, K. Sabbah, M. Rammal, and P. Vaudon, "Synthesis of phased cylindrical arc antenna arrays," *International Journal of Antennas and Propagation*, vol. 2009, Article ID 691625, 5 pages, 2009.

[13] K. Guney, A. Durmus, and S. Basbug, "Antenna array synthesis and failure correction using differential search algorithm," *International Journal of Antennas and Propagation*, vol. 2014, Article ID 276754, 8 pages, 2014.

[14] K. Guney and A. Durmus, "Pattern nulling of linear antenna arrays using backtracking search optimization algorithm," *International Journal of Antennas and Propagation*, vol. 2015, Article ID 713080, 10 pages, 2015.

[15] Y. Han and C. Wan, "Scalable alternating projection and proximal splitting for array pattern synthesis," *International Journal of Antennas and Propagation*, vol. 2015, Article ID 915293, 13 pages, 2015.

[16] T. van Luyen and T. Vu Bang Giang, "Interference suppression of ULA antennas by phase-only control using bat algorithm," *IEEE Antennas and Wireless Propagation Letters*, vol. 16, pp. 3038–3042, 2017.

[17] R. Vescovo, "Reconfigurability and beam scanning with phase-only control for antenna arrays," *IEEE Transactions on Antennas and Propagation*, vol. 56, no. 6, pp. 1555–1565, 2008.

[18] M. Comisso, G. Buttazzoni, and R. Vescovo, "Reconfigurable antenna arrays with multiple requirements: a versatile 3D approach," *International Journal of Antennas and Propagation*, vol. 2017, Article ID 6752108, 9 pages, 2017.

[19] R. Vescovo, "Consistency of constraints on nulls and on dynamic range ratio in pattern synthesis for antenna arrays," *IEEE Transactions on Antennas and Propagation*, vol. 55, no. 10, pp. 2662–2670, 2007.

[20] M. K. Samimi and T. S. Rappaport, "3-D millimeter-wave statistical channel model for 5G wireless system design," *IEEE Transactions on Microwave Theory and Techniques*, vol. 64, no. 7, pp. 2207–2225, 2016.

[21] C. Ling, X. Yin, R. Müller et al., "Double-directional dual-polarimetric cluster-based characterization of 70–77 GHz indoor channels," *IEEE Transactions on Antennas and Propagation*, vol. 66, no. 2, pp. 857–870, 2018.

[22] G. Buttazzoni and R. Vescovo, "Density tapering of linear arrays radiating pencil beams: a new extremely fast Gaussian approach," *IEEE Transactions on Antennas and Propagation*, vol. 65, no. 12, pp. 7372–7377, 2017.

[23] G. Buttazzoni and R. Vescovo, "Power synthesis for reconfigurable arrays by phase-only control with simultaneous dynamic range ratio and near-field reduction," *IEEE Transactions on Antennas and Propagation*, vol. 60, no. 2, pp. 1161–1165, 2012.

[24] R. Vescovo, "Power pattern synthesis for antenna arrays with null constraints in the near-field region," *Microwave and Optical Technology Letters*, vol. 44, no. 6, pp. 542–545, 2005.

Journal of
Engineering

The Scientific
World Journal

International Journal of
Rotating
Machinery

Journal of
Sensors

Advances in
Multimedia

Advances in
Civil Engineering

Journal of
Control Science
and Engineering

Journal of
Robotics

Journal of
Electrical and Computer
Engineering

Advances in
OptoElectronics

VLSI Design

International Journal of
Navigation and
Observation

Modelling &
Simulation
in Engineering

International Journal of
Aerospace
Engineering

International Journal of
Chemical Engineering

International Journal of
Antennas and
Propagation

Active and Passive
Electronic Components

Shock and Vibration

Advances in
Acoustics and Vibration

Hindawi

Submit your manuscripts at
www.hindawi.com